24 keV neutron capture studies in Mo isotopes*

K. Rimawi† and R. E. Chrien
Brookhaven National Laboratory, Upton, New York 11973
(Received 24 November 1976)

Partial cross sections for radiative capture of 24.3 keV neutrons leading to low-lying states of the residual nuclides have been measured for even-A molybdenum targets: ^{92}Mo, ^{94}Mo, ^{96}Mo, and ^{98}Mo. Absolute values of these cross sections were obtained by use of the ^{10}B(n,α) reaction as a reference. These cross sections show correlations to the (d,p) spectroscopic factors for the final states. The expected cross sections are calculated using various models. The single-particle estimates and giant dipole resonance extrapolations are shown to be inadequate. Although a valence neutron transition model can account for the observed correlations, it is inadequate to account for the observed strength. The evidence favors a significant contribution from three quasiparticle components in the capturing states.

[NUCLEAR REACTIONS Neutron capture γ rays, averaged resonance capture 24.3 keV, iron-aluminum beam filter, partial radiative cross sections, correlations between (n,γ) and (d,p), valence transitions, angular correlations, deduced level spins.]

I. INTRODUCTION

Deviations from the statistical model for the radiative neutron capture process have been observed in several regions of the Periodic Table. Such deviations point to the significant contribution of simple reaction mechanisms due to single-particle or doorway-state effects which lead to significant correlations between different reaction widths.[1]

The single-particle effects in the neutron capture process result from single-particle components in both capture and final states that can be linked via $E1$ transitions. This requirement suggests that nuclides in the regions of neutron strength function maxima should be good candidates for such processes. These conditions are met, for example, in the case of the molybdenum isotopes which have a $3p$ single-particle state near threshold and the $g_{9/2}$ neutron shell closed at ^{92}Mo.

For low-energy p-wave resonance capture in ^{92}Mo and ^{98}Mo,[2] it was observed that the Lane and Lynn[3] model of channel capture or Lynn's[4] valence-neutron model roughly predict the measured partial radiative widths for transitions populating low s and d states. However, when these studies were extended to higher resonance energies,[5,6] the model was found to fail to reproduce the measured widths on a quantitative basis.

These studies are extended in the present investigation through the use of a quasimonoenergetic neutron beam at 24 keV on the isotopes ^{94}Mo and ^{96}Mo, as well as ^{92}Mo and ^{98}Mo. The beam has an inherent energy spread larger than the level spacing for these isotopes so that an average of several neutron resonances is obtained. A similar procedure has been exploited by Bollinger and Thomas,[7] using an in-pile target rather than an external beam as is done here. One general conclusion of the in-pile target work is, that for nuclides $A > 150$, the primary γ rays populate final states without regard to the detailed nature of the final state. This nonselective feature of the average resonance capture technique is useful for nuclear spectroscopy. One result of this present investigation is to show that this principle of nonselectivity fails rather badly in the $A \leq 100$ mass region, and in particular near the $3p$ single-particle energy. It is shown that final states of primarily single-particle character are populated more strongly.

II. EXPERIMENTAL ARRANGEMENT AND DATA ANALYSIS

A. Data acquisition

The neutron beam was derived from the High Flux Beam Reactor at Brookhaven National Laboratory through a transmission filter consisting of 22.9 cm iron, 35.6 cm aluminum, 5.1 cm sulfur, and 0.16 cm cadmium. The spectral distribution of the neutron flux transmitted by the filter, shown in Fig. 1 (taken from Ref. 8), is seen to peak at 24.3 keV and to have a full width at half maximum of 2 keV. A neutron flux of 10^6 n/cm^2 sec has been measured at the exit aperture which has the dimensions of 2.54×2.54 cm^2. A complete description of this beam filter is being published separately.[8]

The samples used are described in Table I. These were placed at 45° to the incident neutron

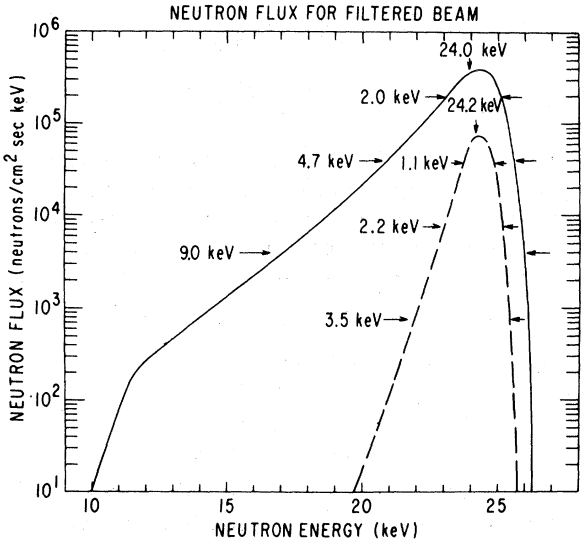

FIG. 1. The energy distribution of the neutron flux available from the HFBR iron-aluminum filter. The solid curve represents a filter of 22.86 cm Fe, 35.56 cm Al, and 5.08 cm S. The dotted curve is for a filter of 68.58 cm Fe, with the other components unchanged.

beam. The ^{94}Mo sample, which had a cylindrical shape, was placed with the axis normal to the plane formed by the neutron beam and the detector. The detector used was a 23 cm^3 planar intrinsic germanium detector which was placed such that the detector-target line formed 90° with the direction of the incident neutron beam.

The pulses generated in the detector were amplified and analyzed using a highly stabilized multichannel analyzer. The spectrum was stored in 4096 channels with a nominal gain of 2 keV per channel. A resolution of 0.1% at 7.5 MeV was typical in the experiment.

B. Data analysis

γ-ray energies and intensities were obtained by fitting the individual peaks assuming a Gaussian shape and determining the peak centroid and area. The energies were determined relative to the background γ-ray lines appearing in the spectrum following capture of thermalized neutrons in iron and hydrogen.

The cross section for the ^{10}B$(n, \alpha\gamma)^7$Li reaction was used as a reference in obtaining the partial radiative capture cross sections. This was done by irradiating composite samples of molybdenum and boron. The boron sample, in powder form, was enriched to 92.8% ^{10}B and had a thickness of 0.0043 atom/b. Values of 5.9175 and 3.4875 b were used for the total and (n, α_1) ^{10}B cross sections, respectively, for the incident neutrons of 24.3 keV.

C. Angular distribution correction

Since the data were taken with the detector at 90° to the incident neutron beam, a correction for the dependence of the γ-ray intensities on the angle must be made when extracting the partial radiative capture cross sections from the data. Since all targets were even-even nuclei, s-wave capture as well as p-wave capture into spin $\frac{1}{2}$ resonances leads to isotropic distributions for the emitted primary γ rays. p-wave resonances with spin $\frac{3}{2}$, however, result in distributions which are angle dependent. These distributions are also functions of the spins of the final states.

The partial cross section for a transition proceeding from a $p_{3/2}$ resonance to a final state of spin J_f may be written in terms of the 90° cross section as

$$\langle\sigma_{3/2}(J_f)\rangle = \sigma_{3/2}(90°)/P(J_f), \quad (1)$$

where

TABLE I. Description of the targets used in this work.

Target	Mass (g)	Thickness [a] (atom/b)	Enrichment (%)	Form
^{92}Mo	49.98	0.0115	97.37	Metallic powder
^{94}Mo	62.411	0.080 [b]	92.03	Metallic cylinder
^{96}Mo	12.37	0.0082	96.76	Metallic powder
^{98}Mo	67.54	0.0065	96.91	Mo O_3 powder
Mo natural	130.69	0.0046		Metallic sheet
^{10}B	3.13	0.0292	92.818	Powder

[a] Thickness in beam direction.
[b] Average; axis of cylinder is perpendicular to plane of beam and detector.

$$P(J_f) = \frac{4\pi I(90^\circ)}{\int I(\Omega) d\Omega} \tag{2}$$

and $I(\Omega)$ is the intensity in the solid angle $d\Omega$. $P(J_f)$ for transitions from an initial state of spin $\frac{3}{2}$ to final states of spin $\frac{1}{2}$, $\frac{3}{2}$, and $\frac{5}{2}$ is found to have the values $\frac{5}{4}$, $\frac{4}{5}$, and $\frac{21}{20}$, respectively.

Since resonances of both spins $\frac{1}{2}$ and $\frac{3}{2}$ contribute to the intensity measured for a certain transition, one can define a multiplier M such that

$$\langle \sigma(n,\gamma) \rangle = M\sigma(90^\circ), \tag{3}$$

where M is given by

$$M = (\sigma_{1/2} + \sigma_{3/2})/(\sigma_{1/2} + P\sigma_{3/2}). \tag{4}$$

In order to evaluate M the relative contributions to the cross section of resonance of different spins must be known. Since in an average capture experiment this is not determined, one has to make certain model-dependent assumptions that would lead to an estimate of M.

III. MODELS FOR THE INTERPRETATION OF THE AVERAGE CROSS SECTION

We use estimates based on various models for the distribution of electric dipole radiative strength with excitation energy. We consider estimates based on the single-particle (Weisskopf) estimates of the radiation strength, on the valence neutron transition model, and on the giant-dipole resonance model, as elaborated by Axel.[9]

A. Single-particle estimate

Neglecting the $M1$ contribution to $\sigma_{1/2}$ which arises from s-wave neutron capture, the average cross section following neutron capture may be expressed as follows:

$$\bar{\sigma}(n,\gamma) = 2\pi^2 \lambda\!\!\!^{-2} \frac{k^2 a^2 \sqrt{E_n}}{1 + k^2 a^2} S^1 \left[\sum_{JS} g_J \frac{\langle \Gamma \rangle_\gamma(J)}{\langle \Gamma \rangle(J)} f_J \right], \tag{5}$$

where S^1 is the p-wave neutron strength function assumed independent of J, the resonance spin. f_J is the fluctuation parameter given by Lynn,[10] $\langle \Gamma \rangle(J)$ is the total width, and $\langle \Gamma \rangle_\gamma(J)$ the partial width corresponding to the emission of the photon γ. All other symbols have their usual meanings.

Assuming $2J+1$ level density dependence and the J independence of the $E1$ photon strength function k_{E1}, defined as

$$k_{E1} = \frac{\langle \Gamma \rangle_\gamma}{E_\gamma^{\,3} D A^{2/3}}, \tag{6}$$

the expression for the average cross section can be reduced to

$$\bar{\sigma}(n,\gamma) = \frac{2\pi \lambda\!\!\!^{-2} (ka)^2}{1 + (ka)^2} \sqrt{E_n}\, (S^1) \frac{D_0}{2(2I+1)} \times A^{2/3} k_{E1} E_\gamma^{\,3} \sum_{JS} \frac{f(J)}{\langle \Gamma(J) \rangle}, \tag{7}$$

where $D_0 = (2J+1)[D(J)]$, I is the target nucleus spin, and the sum extends over resonance spin J and channel spin S. From Eq. (7) it follows that the relative contributions to a transition from spin $\frac{1}{2}$ resonances compared with spin $\frac{3}{2}$ resonances is

$$\sigma_{1/2} : \sigma_{3/2} = f_{1/2} / \langle \Gamma \rangle (\tfrac{1}{2}) : f_{3/2} / \langle \Gamma \rangle (\tfrac{3}{2}). \tag{8}$$

This ratio is used in determining M, the angular distribution correction multiplier.

B. Valence neutron model

Lynn[4] gives the contribution to the partial width of the valence-neutron transition from initial state λ to final state u as

$$\delta\Gamma_{\lambda u} = \frac{16\pi}{9} k_\gamma^{\,3} \bar{e}^2 \theta_\lambda^{\,2} \theta_u^{\,2} I_{\lambda u}^{\,2} A_{\lambda u}^{\,2}, \tag{9}$$

where the radial overlap integral $I_{\lambda u}$ is given by

$$I_{\lambda u} = \int_0^\infty u_\lambda r u_u dr \tag{10}$$

and

$$A_{\lambda u} = \frac{\langle j' I J_\lambda || Y^{(1)} || j'' I J_u \rangle}{(2J_\lambda + 1)^{1/2}}. \tag{11}$$

$\bar{e}$ is the effective charge, θ_λ and θ_u are the reduced dimensionless widths, and u_λ and u_u are the radial wave functions for the initial and final states; $k_\gamma = E_\gamma / \hbar c$.

Using expression (9) for Γ_γ in expression (5) and making the assumption of a $(2J+1)$ dependence for the level density lead to the expression for the valence-neutron transition average cross section for transitions feeding final states u:

$$\bar{\sigma}_u(n,\gamma) = \frac{16\pi^3}{9} \lambda\!\!\!^{-2} \left(\frac{ma^2}{\hbar^2} \right) \left(\frac{(ka)}{1 + (ka)^2} \right) k_\gamma^{\,3} E_n (S^{(1)})^2 \times \left(\frac{D_0}{2J+1} \right) \sum_{J,S} [f(J)/\Gamma(J)] \theta_u^{\,2} I_{\lambda u}^{\,2} A_\lambda^{\,2}, \tag{12}$$

where we have explicitly introduced the single-particle widths $\hbar^2/ma^2$, and the sum extends over spin and channel spin. Note that the expression for the cross section is proportional to the square of the neutron strength function in the valence model approximation.

C. Giant dipole resonance model

Assuming that an $E1$ giant dipole resonance is built on excited states in a manner similar to that built on the ground state (the Brink hypoth-

esis),[9,11] one can estimate the (n,γ) cross section resulting from the tail of this resonance.

The giant dipole (γ,n) cross section is given by[12]

$$\sigma(\gamma,n)=4\pi\hbar c e^2\frac{NZ}{A}\frac{1+0.8x}{Mc^2}\frac{\Gamma_G E^2}{(E_G{}^2-E^2)+\Gamma_G{}^2E^2}, \tag{13}$$

where Γ_G and E_G are the giant resonance width and energy, respectively, and x is the fraction of exchange force present in the nuclear force. Γ_G and E_G were taken from measured (γ,n) cross section.[13]

The (n,γ) cross section is then derived from the (γ,n) cross section by the application of the principle of detailed balance

$$\frac{k_n^2}{g_n}\sigma(n,\gamma)=\frac{k_\gamma^2}{g_\gamma}\sigma(\gamma,n), \tag{14}$$

where g_n and g_γ are the appropriate statistical weight factors.

IV. RESULTS

A. ^{92}Mo$(n,\gamma)^{93}$Mo

The target nucleus ^{92}Mo, with $Z=42$ and $N=50$, has a full $g_{9/2}$ neutron shell. Thus, the ground state and low-lying excited states in the product nucleus ^{93}Mo have large single-particle character corresponding to the $d_{5/2}$, $s_{1/2}$, and $d_{3/2}$ neutron orbitals. Transitions to these states are expected therefore to exhibit large valence neutron components.

In studying capture by resonances up to 23.9 keV, Wasson and Slaughter[6] observed strong correlations of radiative strengths with (d,p) spectroscopic factors, but the correlation with neutron widths, predicted by the valence model, was largely absent.

In the present study a sample of 50 g of metallic Mo was used. The sample was 97.37% ^{92}Mo. The sample thickness as presented to the neutron beam was 0.011 atom/b. A separate run was taken using a sample combined of the ^{92}Mo sample and a ^{10}B sample. This run was used to determine the absolute partial radiative capture cross sections for the ^{92}Mo$(n,\gamma)^{93}$Mo reaction. The spectrum was accumulated for a period of 88 hours. A resolution of 8.8 keV at 7.1 MeV was obtained.

The transition energies and partial cross sections obtained are listed in Table II. While the neutron beam overlaps about seven resonances to varying degrees,[14] the 23.9 keV $p_{3/2}$ resonance is expected to dominate the capture. This is manifested by the observation of the strong transition feeding the $s_{1/2}$ level at 940 keV. This transition was observed to carry 58% of the total capture in the 23.9 keV resonance by Wasson and Slaughter.[6] The expected p-wave spacing is about 900 eV.

TABLE II. ^{92}Mo$(n,\gamma)^{93}$Mo cross sections (in mb) compared with predictions of the statistical, valence, and giant dipole extrapolation models. $E_n=24.3$ keV.

E_γ (keV) [a]	E_x	$\sigma_{\exp(n,\gamma)}$ [b]	J^π	σ_{stat} [c]	σ_v	σ_{GDR}
8090	0	2.8±0.2	$\frac{5}{2}^+$	3.1	3.4	7.2
7150	940	12.3±0.5	$\frac{1}{2}^+$	3.4	3.2	5.8
6600	1490	1.7±0.3	$\frac{3}{2}^+$	2.7	0.8	4.0
6398	1692	0.9±0.2	$\frac{5}{2}^+$	1.5	0.2	
5952	2138	2.3±0.3	$\frac{3}{2}^+$	2.0		
5905	2185	1.0±0.2	$\frac{3}{2}^+$	1.9	0.06	
5695	2395	0.7±0.2	$\frac{3}{2}^+$	1.7	0.05	
5655	2435	0.4±0.2	$\frac{1}{2}^+$	1.7	0.2	
5424	2666	0.3±0.1	$\frac{1}{2}^+$	1.5	0.02	
5390	2700	0.8±0.2	$\frac{1}{2}^+$	1.5	0.7	
5258	2832	0.7±0.3	$\frac{1}{2}^+$	1.4	0.1	
5242	2848	0.6±0.2	$\frac{3}{2}^+$	1.3		

[a] Energy as measured with 2 keV beam spread at 24.3 keV. Approximately ±1 keV systematic error must be included when comparing to thermal neutron capture γ-ray energies.

[b] Corrected for angular correlation. The errors in Tables II–VI do not include fluctuations due to limited sample size.

[c] Using $k_{E1}=1.2\times10^{-9}$ MeV^{-3}.

All levels in ^{93}Mo below 2.83 MeV with spin $\frac{1}{2}$, $\frac{3}{2}$, or $\frac{5}{2}$ seen in charged particle reactions[15,16] are populated in this experiment. In addition the state at 2.141 MeV populated in the resonance neutron capture study of Wasson and Slaughter is also populated. Because of the inherent energy spread of 2 keV in the incident beam, precise γ-ray energy determinations are not possible with the iron filtered beam.

In order to compare the measured cross sections with the values predicted by the valence model, Eq. (12) was used to calculate the valence neutron transition cross section. A value of the p-wave neutron strength function S^1 of 3.3×10^{-4} was used in this calculation.[17] The spectroscopic factors for the low-lying states of ^{93}Mo were taken from Ref. 15. The values calculated are given in Table II. Figure 2 compares the measured cross sections to those calculated for the valence neutron transitions. The table entries as well as the figure point out the qualitative agreement in that states that are expected to be populated strongly in the valence neutron transition, namely, the

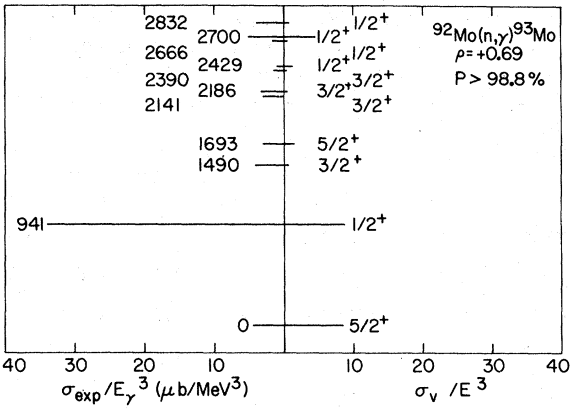

FIG. 2. Measured ^{92}Mo cross sections compared with the valence model calculations. The cross sections are divided by E^3 to remove the phase space factor expected for $E1$ transitions.

$d_{5/2}$ ground state and the $s_{1/2}$ first excited state, are seen to be strongly populated in the experiment.

This agreement is further supported by a calculation of the correlation coefficient for the observed 12 transitions between the measured cross sections and those calculated from the valence transition model. A correlation coefficient of 0.74 is obtained which falls at the 99% point of the normal distribution when testing for zero correlation indicating that such a coefficient is significant.

While such a correlation between the measured $\sigma(n,\gamma)$ and $\sigma_v(n,\gamma)$ suggests that the valence neutron transition contributes significantly to the radiative capture process, a numerical comparison shows that this component accounts for only 35% of the total transition strength and 26% of the transition strength to the 940 keV level. Thus other mechanisms must play a major role in the capture process for ^{92}Mo. This result supports the assertion by Wasson and Slaughter that valence motion does not play a major role in the capture process.

The contribution from the statistical capture is estimated using Eq. (7). A value of $\bar{k}_{E1} = 1.2 \times 10^{-9}$ MeV^{-3} at 7 MeV was used. This value for the photon strength function is obtained from the expression for this function given by Bollinger. A value of $\approx$3 mb is thus calculated for the partial cross section for the transition populating the 940 keV level. This value is also not large enough to explain the observed strength of the transition. Finally, the cross sections for several of the lowest-lying levels are also calculated using experimental parameters for the giant dipole resonance as obtained from photonuclear work on Mo isotopes[13] and the Brink hypothesis. In this case, and in fact for all the Mo isotopes, the giant dipole resonance extrapolated cross sections generally exceed the calculated cross sections of the valence model or the various statistical estimates using empirical photon strength functions. In general the experimental values are also exceeded, an exception being the $s_{1/2}$ state of ^{93}Mo at 940 keV. In none of these estimates, whether based on single-particle or giant dipole resonance approximations, is the calculated strength sufficient. The sum of the calculated valence neutron cross section and the estimated statistical contribution to the transition cross section amounts to only about $\frac{1}{2}$ of the measured cross section for this transition.

Even though a single resonance dominates the capture at 24 keV in this experiment, the enhanced transition strength *cannot* be explained as a Porter-Thomas fluctuation. It is 10 times larger than the mean of all the other transition strengths and is thus not consistent with the χ^2 distribution with $\nu = 1$.

B. ^{94}Mo$(n,\gamma)^{95}$Mo

With the addition of two neutrons to the $d_{5/2}$ orbital, the level density for low-lying states in ^{95}Mo is expected to be higher than in the case of ^{93}Mo, and the single-particle strength split among these levels. This was observed in the (d,p)[15,16] and (d,t)[16] studies.

The expected p-wave resonance spacing for ^{94}Mo is ~550 eV, as calculated from Ref. 17.

The sample used was in the form of a metallic cylinder which weighed 62.41 g with a height of 2.26 cm and a diameter of 2.0 cm. The sample was enriched to 92.03% in ^{94}Mo. The highest impurity was ^{95}Mo which formed 5.18% of the sample. The other Mo isotopes were present in quantities of less than 1% each. The sample was irradiated in the 24.5 keV beam for a period of 96 hours. Figure 3 shows the high energy portion of the observed spectrum. Strong transitions are seen to the lowest six states in ^{95}Mo. Since the level spins reported in the (d,p) and (d,t) studies referred to above often disagreed for $l_n = 2$, it was necessary to attempt an independent determination from the (n,γ) reaction. An attempt to obtain such information from thermal neutron capture using a beam derived through a 35.6 cm Bi crystal filter proved unsuccessful, as the spectrum was dominated by capture in ^{95}Mo impurity. Another attempt at observing capture γ rays following capture in low-energy resonances in ^{94}Mo was equally unsuccessful since the time of flight spectrum showed a peak to background ratio of 0.25 (at 109 eV) while the γ spectrum showed no strong transitions above background. The strong transitions observed at

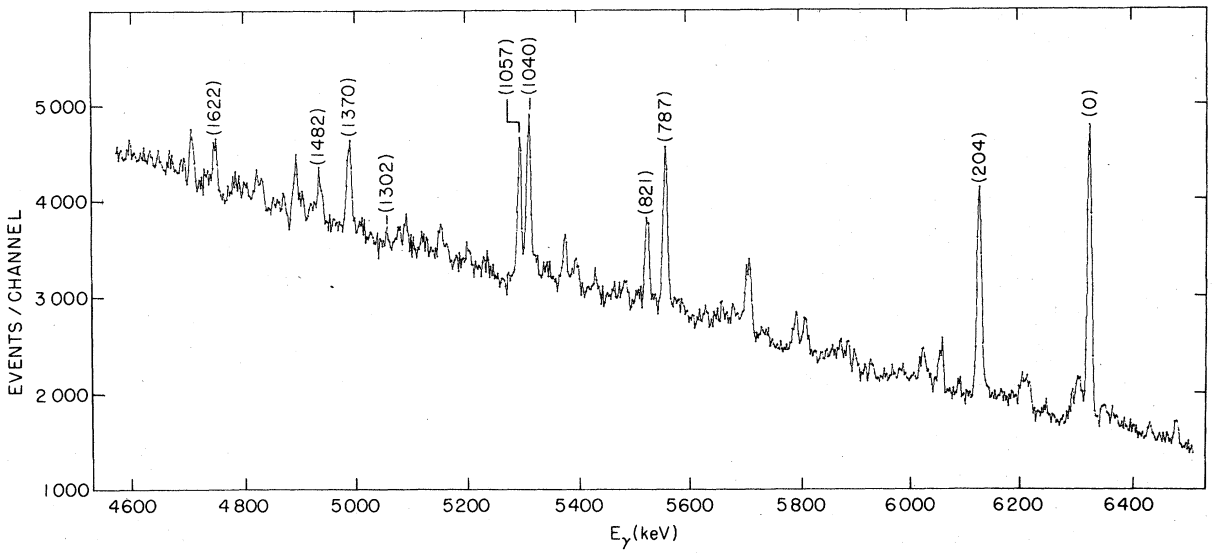

FIG. 3. A portion of the spectrum for ^{94}Mo$(n,\gamma)^{95}$Mo, resulting from 24.3 keV neutron capture. The peaks are two-escape peaks labeled with the excitation energy, in keV, of the ^{95}Mo final state. Unlabeled peaks are either background peaks, or one-escape or full energy peaks from ^{95}Mo transitions.

24.3 keV neutron capture, however, suggested the study of the angular distribution of these γ rays in order to derive such information on the spin of the states populated by these transitions. The spectrum was measured, thus, at an angle of 135° in addition to the 90° measurement.

Since the target nucleus has a 0^+ ground state, p-wave capture would lead to $\frac{1}{2}^-$ and $\frac{3}{2}^-$ states that can feed the low-lying s-wave or d-wave levels via $E1$ transitions. The angular dependence would arise from capture via $E1$ transitions in the $p_{3/2}$ resonances only, while $p_{1/2}$ resonances lead to isotropic distribution. For pure $p_{3/2}$ capture the observed γ-ray ratios $R(J_f)$ for the transition intensity observed at 135° to that observed at 90° leading to a final state J_f are

$$R(\tfrac{1}{2})=0.70, \quad R(\tfrac{3}{2})=1.38, \quad \text{and } R(\tfrac{5}{2})=0.93 .$$

The added $p_{1/2}$ capture will substantially modify these ratios (to values closer to 1.0) for low-lying states with spin $\frac{1}{2}$ or $\frac{3}{2}$ but will not affect transitions feeding $\frac{5}{2}$ low-lying states. One can estimate the magnitude of the effect of capture in $p_{1/2}$ resonances on $R(J_f)$ by the use of the statistical model assumptions discussed in Sec. II above. This leads to the modified values for $R(J_f)$

$$R(\tfrac{1}{2})=0.79, \quad R(\tfrac{3}{2})=1.22, \quad \text{and } R(\tfrac{5}{2})=0.93 .$$

The observed intensities of the two runs were normalized in such a way that the ratio R for the ground state transition was equal to the predicted value of 0.93. This transition was used for normalization of the two runs since the ground state is known to be a $d_{5/2}$ state which is populated only by transitions from $p_{3/2}$ resonances. The results obtained for the six highest energy transitions are given in Table III, where the spins assigned are those consistent with the calculated ratios. Shown also in the table are the spins given to these states in Refs. 15 and 16. The table also lists the spins obtained by Marsh and Mayer[19] by studying the conversion electron and γ spectra following the decay of ^{95}Tc. As seen in the table, the ratios R for spin $\frac{1}{2}$ final states agree rather well with the value predicted from the statistical model assumptions. However, the ratios for transitions feeding the $\frac{3}{2}$ final states are smaller; the comparison suggests that these states are predominantly fed by transitions from $p_{1/2}$ resonances. This may be due to the Porter-Thomas[20] fluctuations, since only a few resonances are expected to contribute to the capture process in the 2.0 keV averaging interval.

The partial capture cross sections were obtained by comparing the transition strength for the ^{94}Mo$(n,\gamma)^{95}$Mo to that of the ground state transition following capture in ^{98}Mo. This was done by running a natural Mo sample for this purpose. The partial cross sections obtained are given in Table IV together with the γ-ray energies and the excitation energies of the levels they feed.

Table IV shows that the six transitions at the high energy end of the spectrum appear to be enhanced when compared with the average transition strength for all observed transitions. Figure 4 is a plot of the relative reduced transition strength $\sigma(n,\gamma)/E_\gamma^3$ for transitions with $E_\gamma > 4.8$ MeV. Ex-

TABLE III. Ratios of the capture cross sections at 135° to 90° for ^{94}Mo$(n,\gamma)^{95}$Mo, with deduced spin assignments.

	This experiment			Ref. 15		Ref. 16		Ref. 19	
E_γ (keV)	E_x	R	J	E_x	J	E_x	J	E_x	J
7390.6	0	0.93 ± 0.04	$\frac{5}{2}$	0	$\frac{5}{2}$	0	$\frac{5}{2}$	0	$\frac{5}{2}$
7186.8	203.8	1.03 ± 0.05	$\frac{3}{2}$	204	$(\frac{3}{2})$	205	$(\frac{5}{2})$	204.12	$\frac{3}{2}$
6603.6	787.0	0.82 ± 0.07	$\frac{1}{2}$	789	$\frac{1}{2}$	787	$\frac{1}{2}$	786.19	$\frac{1}{2}$
6569.6	821.0	1.07 ± 0.11	$\frac{3}{2}$	823	$(\frac{5}{2})$	822	$(\frac{3}{2})$	820.61	$\frac{3}{2}$
6350.6	1040.0	0.81 ± 0.06	$\frac{1}{2}$	1044	$\frac{1}{2}$	1041	$\frac{1}{2}$	1039.25	$\frac{1}{2}$
6333.6	1057.0	0.87 ± 0.07	$\frac{5}{2}$			1059	$(\frac{5}{2})$	1056.79	$\frac{5}{2}$

cluding the six transitions referred to above, the γ-ray transition strength appears to have an E_γ^3 dependence. We can examine the assumption that this enhancement of the high energy transitions is attributed to the valence neutron transition mechanism. The spectroscopic factors of Ref. 15 were used in evaluating this contribution to the different transitions, along with a value of $(5.4 \pm 1.5) \times 10^{-4}$ for the p-wave strength function.[17] The values obtained for the 10 highest energy transitions observed are given in Table IV. The valence model is seen to account for 31% of the ground state transition and 55% of the transition to the first $s_{1/2}$ state. The valence contribution, however, to the first $d_{3/2}$ state is less than 1% of the observed strength.

TABLE IV. Cross sections (in mb) for ^{94}Mo$(n,\gamma)^{95}$Mo compared with predictions of the statistical, valence, and giant dipole extrapolation models. $E_n = 24.3$ keV.

E_γ (keV) [a]	E_x	$\sigma_{\exp}(n,\gamma)$ [b]	J^π	σ_{stat} [c]	σ_v	σ_{GDR}
7391	0	10.9 ± 1.0	$\frac{5}{2}^+$	2.6	3.4	10.4
7187	204	9.1 ± 1.1	$\frac{3}{2}^+$	3.7	0.07	13.6
6604	787	4.8 ± 0.6	$\frac{1}{2}^+$	2.8	2.7	9.1
6570	821	4.0 ± 0.5	$\frac{3}{2}^+$	2.8	1.0	
6351	1040	4.5 ± 0.6	$\frac{1}{2}^+$	2.5	1.2	
6334	1057	4.0 ± 0.6	$\frac{5}{2}^+$	1.6	•••	
6089	1302	0.1 ± 0.2	$\frac{1}{2}^+$	2.2	0.02	
6021	1370	1.0 ± 0.2	$\frac{5}{2}^+$	1.4	0.07	
5963	1428	2.0 ± 0.3	$\frac{5}{2}^+$	2.1	0.05	
5769	1622	1.8 ± 0.5	$\frac{3}{2}^+$	1.9	0.3	

[a] Energy as measured with 2 keV beam spread at 24.3 keV. Approximately ± 1 keV systematic error must be included when comparing to thermal neutron capture γ-ray energies.

[b] Corrected for angular correlation.

[c] $k_{E1} = 1.2 \times 10^{-9}$.

The valence model predictions are compared with the measured cross sections of Fig. 5. A correlation coefficient of 0.62 is obtained for the two sets of data. This falls at the 97% point of the distribution obtained for a zero correlation hypothesis. This indicates a significant contribution from nonstatistical effects to the radiative capture process in this case.

C. ^{96}Mo$(n,\gamma)^{97}$Mo

Information on the levels of ^{97}Mo has been obtained through (d,p) studies. Hjorth and Cohen[18] studied this reaction with a resolution which did not separate the proton groups feeding close levels. A higher resolution study by Ajzenberg-Selove and Maxman[21] reports 17 levels up to 2.56 MeV in ^{97}Mo but no spins are assigned.

A more recent (d,p) study by Medsker and Yntema[22] reports levels up to 4 MeV with a resolution of 15 keV. Over 80 levels were reported in this study, and l_n was determined for most of the lev-

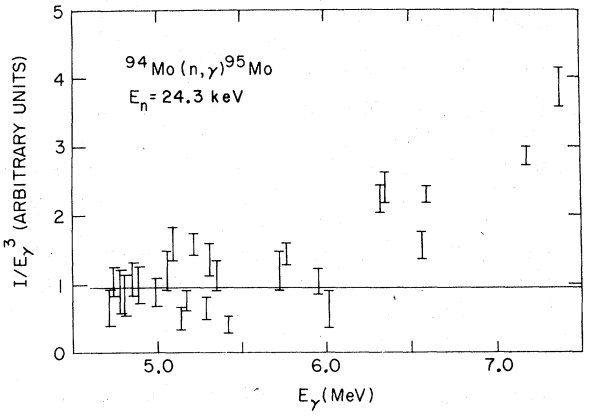

FIG. 4. A plot of relative reduced transition strengths (I_γ/E^3) for ^{94}Mo$(n,\gamma)^{95}$Mo, for $E_\gamma > 4.8$ MeV. The enhancement of the high energy transitions over an expected E^3 dependence is evident.

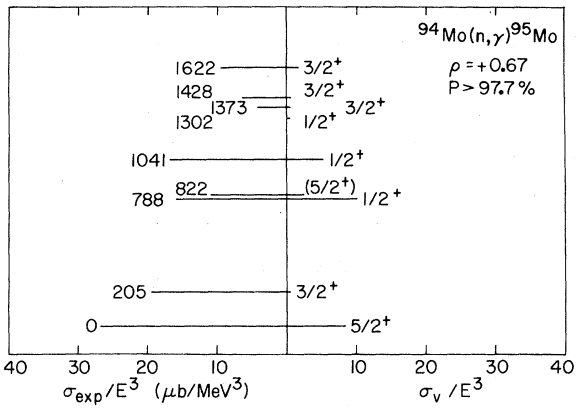

FIG. 5. Capture cross sections for ^{94}Mo$(n,\gamma)^{95}$Mo compared with predicted valence model cross sections.

els. However, except for s-wave neutron transfer, few unique level spins were assigned. The observation of about 40 levels with $l_n=2$ reflects the fragmentation of the single-particle strength resulting from the additional neutrons to the nucleus.

We expect a p-wave resonance spacing for ^{96}Mo of ~390 eV, from the data available in Ref. 17.

The sample used in this study consisted of 12 g of metallic powder enriched to 96.76% of ^{96}Mo. The spectrum was accumulated for a period of 96 hours. The energies obtained for γ rays with energies greater than 4.8 MeV are listed in Table V. The excitation energy for the levels fed by these transitions is also listed in the table.

The cross sections were determined from the measured intensities for the transitions seen in the spectrum. The normalization constant was obtained from the natural sample run by comparison to the ground state transition in ^{99}Mo following capture in ^{98}Mo. The partial cross sections obtained are listed in Table V. Where the spin of the final state is not known, the cross section value as measured at 90° is entered in the table.

In order to compare the measured cross sections with those calculated from the valence model, one needs to know the spins of the final states. In order to determine the spins of $l_n=2$ states, the thermal capture was studied as well as capture in the 131 eV resonance. In both cases the capturing states are $\frac{1}{2}^+$. These states feed low-lying $l_n=2$ states via a mixture of $M1$ and $E2$ transitions in the case of spin $\frac{3}{2}^+$ final states and via pure $E2$ transitions in the case of $\frac{5}{2}^+$ states. The average $M1$ and $E2$ strength was determined for capture in seven s-wave resonances in ^{92}Mo by Wasson and Slaughter.[6] Assuming similar ratios to hold in the case of capture in ^{96}Mo, one can estimate the $E2$ to $M1$ transition strength ratio to be

TABLE V. Cross sections (in mb) for ^{96}Mo$(n,\gamma)^{97}$Mo compared with predictions of the statistical, valence, and giant dipole extrapolation models. $E_n=24.3$ keV.

E_γ (keV) [a]	E_x	$\sigma_{\exp}(n,\gamma)$ [b]	J^π	σ_{stat} [c]	σ_v	σ_{GDR}
6844	0	3.3±0.5	$\frac{5}{2}^+$	2.1	0.8	8.9
6364	480	2.9±0.6	$\frac{3}{2}^+$	2.6		9.5
6164	680	4.0±0.9	$\frac{1}{2}^+$	2.4	2.2	8.2
6124	720	5.6±0.9	$\frac{3}{2}^+$	2.3	0.5	
5956	888	1.2±0.4	$\frac{1}{2}^+$	2.1	0.1	
5749	1095	1.9±0.5				
5579	1265	3.4±0.6	$\frac{3}{2}^+$	1.8	0.4	
5562	1282	1.2±0.4	$\frac{3}{2}^+$	1.7	0.1	
5327	1517	1.4±0.4	$\frac{3}{2}^+$	1.5	0.03	
5294	1550	0.3±0.4	$\frac{1}{2}^+$	1.5	0.2	
5118	1726	1.5±0.4	$\frac{1}{2}^+ + (\frac{3}{2},\frac{5}{2})^+$	•••	•••	
4997	1847	1.9±0.8	$\frac{1}{2}^+$	1.3	0.1	
4884	1960	0.4±0.4	$(\frac{3}{2},\frac{5}{2})^+$	•••	•••	
4812	2032	1.2±0.4	$\frac{1}{2}^+$	1.1	0.3	

[a] Energy as measured with 2 keV beam spread at 24.3 keV. Approximately ± 1 keV systematic error must be included when comparing to thermal neutron capture γ-ray energies.

[b] Corrected for angular correlation: When spin of final state is not known, $\sigma(90°)$ has been listed.

[c] Using $k_{E1}=1.2\times10^{-9}$ MeV^{-3}.

of the order of 20%, implying that the stronger transitions are most likely $M1$ transitions, leading to a spin of $\frac{3}{2}^+$ for the low-lying state fed by these strong transitions.

Using the above argument states below 2 MeV were assigned unique spins when possible, and the valence neutron contribution was calculated. A value of $S^1=(4.5\pm1.0)\times10^{-4}$ was used in the calculation.[17] The spectroscopic factors were taken from Ref. 22 as $S_{lj}=G_{lj}/(2J_f+1)$. These values were used to compute valence cross sections and are given together with the measured cross sections in Table V and shown in Fig. 6.

A correlation coefficient of 0.49 is obtained for the two sets of data. This falls at the 95% point of the distribution for uncorrelated sets. The absence of the dominant transitions in this case as opposed to the situation in capture in ^{92}Mo and ^{94}Mo seems to reflect the absence of the large single-particle component in these transitions due to the greater fragmentation of the single-particle strength. The observed strength in general does not seem to exceed the expected strength estimated

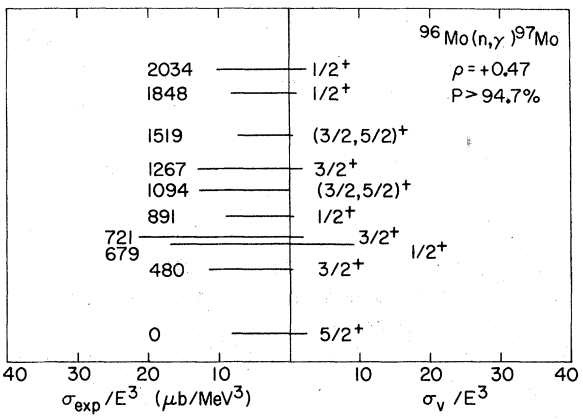

FIG. 6. Capture cross sections for ^{96}Mo$(n,\gamma)^{97}$Mo compared with predicted valence model cross sections.

from the contributions of the valence plus the statistical components.

D. ^{98}Mo$(n,\gamma)^{99}$Mo

The valence neutron contribution to the capture process is expected to show up more strongly in ^{98}Mo than for the other Mo isotopes. ^{98}Mo has a larger p-wave neutron strength function,[17] (7.0 $\pm$1.0) $\times 10^{-4}$ in addition to having a $d_{5/2}$ minor shell closure leading to a large single-particle strength for the low-lying states. This is true, in particular, in the case of the $s_{1/2}$ ground state of ^{99}Mo which has a spectroscopic factor of 0.67.[15] Furthermore, ^{98}Mo has the smallest level spacing of the isotopes studied in this experiment, thus leading to better averaging of the capture process over more resonances and thus reducing the statistical fluctuation effects; the p-wave resonance spacing from Ref. 5 is about 300 eV.

TABLE VI. Cross sections (in mb) for ^{98}Mo$(n,\gamma)^{99}$Mo compared with predictions of the statistical, valence, and giant dipole extrapolation models. E_n = 24.3 keV.

E_γ (keV) [a]	E_x	$\sigma_{exp}(n,\gamma)$ [b]	J^π	σ_{stat} [c]	σ_v	σ_{GDR}
5947	0	7.0 ± 0.3	$\frac{1}{2}^+$	2.5	4.3	12.0
5848	99	1.1 ± 0.4	$\frac{5}{2}^+$	1.4	0.8	7.4
5596	351	1.7 ± 0.3	$\frac{3}{2}^+$	1.6	0.2	9.1
5422	525	1.5 ± 0.2	$\frac{1}{2}^+$	1.9	0.2	
5399	548	1.8 ± 0.3	$\frac{3}{2}^+$	1.4	0.8	
5334	613	0.7 ± 0.2	$\frac{5}{2}^+$	1.1	0.05	
5316	631	1.2 ± 0.2	$\frac{3}{2}^+$	1.4		
5155	792	2.5 ± 0.3	$\frac{3}{2}^+$	1.2	0.05	
5058	889	1.5 ± 0.6	$\frac{3}{2}^+$	1.2	0.14	
5044	903	0.7 ± 0.2	$(\frac{1}{2}^+)$	1.5	0.08	
5036	911	0.7 ± 0.2	$(\frac{3}{2}^+)$	1.5	0.01	
5001	946	0.6 ± 0.2	$(\frac{5}{2}^+)$	0.9		

[a] Energy as measured with 2 keV beam spread at 24.3 keV. Approximately ± 1 keV systematic error must be included when comparing to thermal neutron capture γ-ray energies.

[b] Corrected for angular correlation.

[c] Using $k_{E1} = 1.2 \times 10^{-9}$ MeV^{-3}.

The dominance of the valence neutron contribution to the transitions feeding the low-lying states had been earlier suggested by Mughabghab *et al.*[2] for neutron capture in the low-lying p-wave resonances in ^{98}Mo. Subsequent study of neutron capture in higher energy p-wave resonances,[5] however, showed the inadequacy of the model for quantitative predictions of radiative widths.

The sample used in this investigation consisted of 67.6 g of MoO_3 in powder form. A portion of the γ-ray spectrum obtained is shown in Fig. 7. The γ-ray energies and measured partial cross sections obtained from this spectrum are listed in Table VI. The cross sections were normalized relative to the ^{10}B$(n,\alpha\gamma)^7$Li cross section.

Table VI also lists the excitation energy of the low-lying levels in ^{99}Mo fed by primary transitions observed in this experiment. All levels below 1 MeV given in the (d,p)[15] and (d,t)[16] studies as $l_n = 0$ or $l_n = 2$ states are seen to be populated. In addition, the level at 631 keV, which has not been reported in the charged particle reactions, is also populated. Evidence for the existence of this level comes also from the resonance neutron capture study of Chrien *et al.*[5]

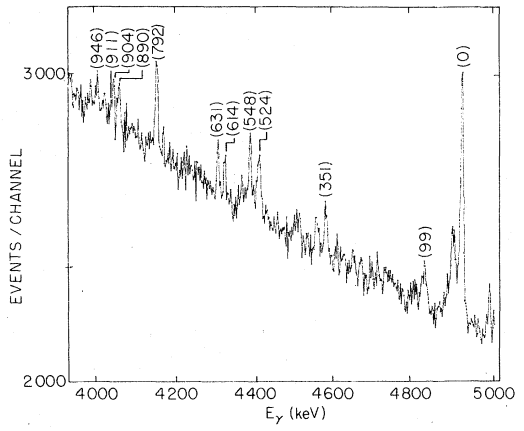

FIG. 7. A portion of the γ-ray spectrum from ^{98}Mo$(n,\gamma)^{99}$Mo. The peaks are labeled as in Fig. 3. Note the appearance of the level at 631 keV, not seen in previous charged particle reaction data, but seen in resonance neutron capture γ-ray work.

The γ-ray spectrum is seen to be dominated by the ground state transition. This dominance is in accord with the predictions of the valence neutron model. The contributions to states of known spin from this component are also listed in Table VI. This component is seen to contribute 61% of the ground state transition strength, the remainder could be attributed to other mechanisms. The statistical component is computed to be 1.8 mb and contributes 26% of the transition strength. The sum of these two components is almost sufficient to explain the observed cross section.

The other partial cross sections predicted from the valence model calculation are compared with the measured values in Fig. 8. A correlation coefficient of 0.97 is obtained for the two sets of data, which falls at the 99% confidence level and once again suggests the significant role played by nonstatistical effects in the capture process.

E. Total capture cross section

The total capture cross section was measured for ^{98}Mo by measuring the intensities of the low-energy γ-ray transitions of energies 740 and 778 keV. These lines are emitted following the β decay of ^{99}Mo to ^{99}Tc.

The ^{98}Mo sample, combined with a ^{10}B sample, was irradiated for a period of 68 hours. The γ spectrum was recorded during this run and the 478 keV line produced in the ^{10}B$(n, \alpha\gamma)^{7}$Li reaction was used to measure the neutron flux. The sample, in the same geometry, was allowed to decay ($t_{1/2}$ = 66 h) with the beam off for a period of 47 hours. The decay spectrum was also recorded.

The cross section was determined from the observed intensities of the 740 keV line, both with the beam on and off. The 778 keV line, which overlaps a line emitted from neutron capture in ^{95}Mo, was used to determine the total capture cross section in the decay run only.

The branching ratios given by Gardulski and Wiedenbeck[23] were used. A total cross section value of 125 ± 15 mb was obtained for the average capture at 24.3 keV in ^{98}Mo.

The ground state transition contributes only 5.6% of the total capture cross section. This value significantly differs from the value obtained by Mughabghab *et al.*[2] for the resonance capture in the resonances at 429, 612, and 818 eV where the contribution of this transition was found to be 20.1, 18.8, and 18.6% of the total capture in the three resonances, respectively.

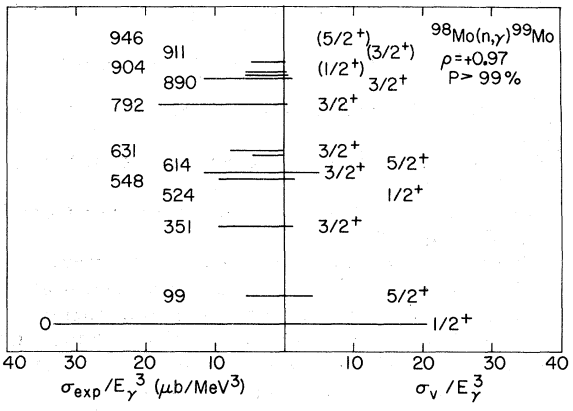

FIG. 8. Capture cross sections for ^{98}Mo$(n,\gamma)^{99}$Mo as compared with valence model predictions.

V. CONCLUSIONS

In summary, the Mo isotopes studied in this experiment exhibit, with varying degrees, a correlation between the measured cross sections for the (n,γ) process and those calculated from a simple single nucleon transition. This correlation is seen to be strongest for ^{98}Mo where it is expected to be strongest and is smallest in ^{96}Mo where the fragmentation of the single-particle strength among low-lying states is largest. This consistency with the model predictions forms significant evidence for the presence of the valence transition contribution to the capture process.

The calculated valence transition contribution, however, is not sufficient to explain the enhancement of the transitions to certain final states whether they exhibit large single-particle character as in the case of the $s_{1/2}$ first excited state in ^{93}Mo, or in the case of states with weak single-particle character as in the $d_{3/2}$ state in ^{95}Mo. These enhanced transitions point to the existence of other simple processes which contribute significantly to the capture process, such as two step doorway-state effects. Soloviev[24] has calculated the expected three quasiparticle state in ^{93}Mo which may be expected to contribute to the resonances near the neutron binding energy. He finds $\frac{3}{2}$ levels of the form $(d_{5/2}+d_{5/2}+f_{5/2})$, $(d_{5/2}+g_{9/2}+h_{11/2})$, $(p_{3/2}+d_{5/2}+d_{5/2})$, and $(d_{5/2}+p_{3/2}+s_{1/2})$. These states, at E_x = 7.5 to 8.5 MeV are expected to be fragmented among the fine structure resonances and thus contribute strongly to $E1$ strengths to low-lying $s_{1/2}$ and $d_{5/2}$ final states. The presence of this admixture can easily explain the quantitative failure of the valence model and yet retain the observed final state correlations reported here.

In calculating the (n,γ) cross section from the measured (γ,n) cross section, using the detailed balance principle, one obtains an overestimate of

the observed cross sections, except for the strongly enhanced transition to the 941 keV $s_{1/2}$ state of ^{93}Mo. These calculated values are shown for the three highest energy transitions in each nucleus in the appropriate tables listing the measured cross sections.

While the degree of averaging in those isotopes is limited by the level spacings of 300 to 900 eV from ^{98}Mo to ^{92}Mo, the overestimates are observed for a number of independent transitions in each of the four isotopes. Thus the overestimate of the cross section by the giant dipole resonance extrapolation is well established in this mass region.

This observation is consistent with that pointed out by Bollinger[11] that the predictions of the giant dipole resonance model are generally observed to be about a factor of 2 higher than the observed transition strength. This consistent discrepancy raises some question about the validity of the giant resonance extrapolation.

Recently, for example, Bergqvist[25] has pointed out that the same discrepancy exists for ^{198}Au; a nuclide for which careful measurements exist for a range of incident neutron energies from thermal up to 2.5 MeV. For gold the extrapolated giant dipole resonance Lorentzian function predicts a photon strength function larger by a factor of about 2.7 than is actually observed. Furthermore, a very marked non-Lorentzian shape has been observed in the region for $3 > E_\gamma > 8$ MeV. These observations, combined with our present results, indicate strongly that the Lorentzian extrapolation is inadequate to predict photon strength functions at or below an excitation corresponding to the neutron binding energy. It will certainly be useful to extend measurements such as these to other mass regions to explore the behavior of the discrepancy.

Note added in proof. We give explicit values for reaction Q values, derived from our ground state transition energies. These are as follows: ^{92}Mo(n,γ), 8066 ± 2 keV; ^{94}Mo(n,γ), 7367 ± 2 keV; ^{96}Mo(n,γ), 6820 ± 2 keV; and ^{98}Mo(n,γ), 5923 ± 2 keV.

---

*Work performed under the auspices of the U.S. Energy Research and Development Administration.

†Present address: New York State Health Department, 677 South Salina Street, Syracuse, New York 13202.

[1]A. M. Lane, in *Neutron Capture γ-Ray Spectroscopy* (Reactor Centrum Nederlands, Petten, The Netherlands, 1975).

[2]S. F. Mughabghab, R. E. Chrien, O. A. Wasson, G. W. Cole, and M. R. Bhat, Phys. Rev. Lett. 26, 1118 (1971).

[3]A. M. Lane and J. E. Lynn, Nucl. Phys. 17, 586 (1960).

[4]J. E. Lynn, *The Theory of Neutron Resonance Reactions* (Clarendon, Oxford, 1968), p. 330.

[5]R. E. Chrien, G. W. Cole, G. G. Slaughter, and J. A. Harvey, Phys. Rev. C 13, 578 (1976).

[6]O. A. Wasson and G. G. Slaughter, Phys. Rev. C 8, 297 (1973).

[7]L. M. Bollinger and G. E. Thomas, Phys. Rev. C 2, 1951 (1970).

[8]R. C. Greenwood and R. E. Chrien, Nucl. Instrum. Methods (to be published).

[9]P. Axel, Phys. Rev. 126, 671 (1962). Also, D. M. Brink, Ph.D. thesis, Oxford University, 1955 (unpublished).

[10]See Ref. 4, p. 229.

[11]L. M. Bollinger, in *Photonuclear Reactions and Applications*, edited by B. L. Berman (National Technical Information Service, U. S. Department of Commerce, Springfield, Virginia, 1973), Vol. II, p. 783 (CONF-73031).

[12]E. Hayward, in *Nuclear Structure and Electromagnetic Interactions*, edited by N. MacDonald (Plenum, New York, 1965).

[13]R. Bergere, H. Beil, P. Carlos, A. Lepretre, and A. Veyssiere, in *Photonuclear Reactions and Applications*, edited by B. L. Berman (see Ref. 11), Vol. II, p. 525.

[14]O. A. Wasson, B. J. Allen, R. R. Winters, R. L. Macklin, and J. A. Harvey, Phys. Rev. C 7, 1532 (1973).

[15]J. B. Moorhead and R. A. Moyer, Phys. Rev. 184, 1205 (1969).

[16]R. C. Diehl, B. L. Cohen, R. A. Moyer, and L. Goldman, Phys. Rev. C 1, 2132 (1970).

[17]*Resonance Parameters*, compiled by S. F. Mughabghab and D. I. Garber, Brookhaven National Laboratory Report No. BNL-325 (National Technical Information Service, Springfield, Virginia, 1973), 3rd ed.

[18]S. A. Hjorth and B. L. Cohen, Phys. Rev. 135, 920 (1964).

[19]K. V. Marsh and R. A. Meyer, Bull. Am. Phys. Soc. 19, 473 (1974).

[20]C. E. Porter and R. G. Thomas, Phys. Rev. 104, 483 (1956).

[21]F. Ajzenberg-Selove and S. H. Maxman, Phys. Rev. 150, 1011 (1966).

[22]L. R. Medsker and J. L. Yntema, Phys. Rev. C 9, 664 (1974).

[23]P. L. Gardulski and M. L. Wiedenbeck, Phys. Rev. C 9, 262 (1974).

[24]V. G. Soloviev, in *Neutron Capture γ-Ray Spectroscopy* (see Ref. 1), p. 99.

[25]I. Bergqvist, quoting work of E. D. Earle, I. Bergqvist, and L. Nilsson, in *Proceedings of the International Conference on Interaction of Neutrons with Nuclei, Lowell, Massachusetts* (National Technical Information Service, U.S. Department of Commerce, Springfield, Virginia, 1976), p. 99 (CONF-760715 P-1).